J Physiol 588.2 (2010) pp 301–314

The Journal of Physiology

Kinetic properties of mechanically activated currents in spinal sensory neurons

François Rugiero, Liam J. Drew and John N. Wood

Molecular Nociception Group, Wolfson Institute for Biomedical Research, University College London, Gower Street, London WC1E 6BT, UK

Dorsal root ganglion neurons *in vitro* express a number of types of mechanically activated currents that are thought to underlie somatic mechanosensory transduction *in vivo*. We have studied the inactivation properties of these currents to assess how they might influence the electrophysiological responses of dorsal root ganglion (DRG) neurons to mechanical stimulation. We show that the speed of ramp-like mechanical stimulation determines the dynamics of mechanically activated current responses and hence the type of DRG neuron most likely to be activated. We also show that both rapidly and slowly adapting currents inactivate as a function of membrane stretch. However, the rapidly adapting current inactivation time course is mainly dependent on channel opening whilst slowly adapting current kinetics are dependent on membrane stretch. In response to repeated stimulation, slowly adapting currents inactivate less and recover more quickly than rapidly adapting currents. Therefore, vibratory stimuli tend to inactivate rapidly adapting currents whilst static stimuli tend to inactivate slowly adapting currents. Current clamp experiments show that, physiologically, the response of different types of sensory neurons is dictated primarily by the static or dynamic nature of the mechanical stimulus and the interplay between voltage-gated and mechanically gated ion channels expressed in these neurons.

(Received 1 October 2009; accepted after revision 24 November 2009; first published online 30 November 2009)
Corresponding author F. Rugiero: Wolfson Institute for Biomedical Research, University College London, Cruciform Building, Wing 3.1, Gower Street, London WC1E 6BT, UK. Email: f.rugiero@ucl.ac.uk

Abbreviations DRG, dorsal root ganglion; IA, intermediately adapting; MA, mechanically activated; RA, rapidly adapting; SA, slowly adapting.

Introduction

Somatosensory ganglia contain phenotypically diverse populations of neurons that encode specific aspects of thermal, chemical and mechanical stimuli. The vast majority of dorsal root ganglion (DRG) and trigeminal ganglion neurons are mechanosensitive, but different subtypes of neurons (e.g. proprioceptors, touch receptors, hair follicle receptors and nociceptors) vary markedly in their sensitivity to mechanical displacement and the pattern of firing evoked by a given mechanical stimulus (Lewin & Moshourab, 2004).

The mechanically evoked firing patterns that characterise DRG neuronal subtypes are likely to be determined by an interaction between factors intrinsic and extrinsic to the neuron. The extrinsic factors include the position of the sensory terminal in the innervated tissue and whether or not it is associated with a specialised end organ that may anchor the fibre, act as a mechanical filter or itself be mechanosensitive. The intrinsic factors include the complement of voltage-gated ion channels expressed and, critically, the properties of the primary mechanotransducing ion channels expressed at the peripheral terminal.

The molecular identity of these mechanotranducers is as yet unknown. However, studies of mechanosensitive ion channels in cultured sensory neurons suggest that the transducers are voltage independent, either non-selective cation channels (Drew *et al.* 2002; Hu & Lewin, 2006) or Na^+-selective channels (Hu & Lewin, 2006). Recent results have shown that it is very unlikely that these channels are homomeric TRP channels of the TRPV1–4, M8 and A1 varieties (Rugiero & Wood, 2009). Currents mediated by these channels can be separated on the basis of their decay kinetics (Drew *et al.* 2002, 2004; Hu & Lewin, 2006): rapidly adapting (RA) currents decline very quickly (<20 ms), slowly adapting (SA) currents are persistent (in a 100 ms time frame) and a third population of mechanically activated (MA) currents decay at an intermediate rate (intermediately adapting, IA). RA currents have a low threshold of activation and are the major MA currents of large mechanosensitive neurons while SA

DOI: 10.1113/jphysiol.2009.182360

and IA currents are mainly found in nociceptors (Drew *et al.* 2002, 2004, 2007*b*; Hu & Lewin, 2006). Furthermore, blocking all types of MA channels in DRG neurons affects both high and low threshold mechanosensation (Drew & Wood, 2007*a*) whilst the pharmacological blockade of SA currents in nociceptors by the conopeptide NMB1 has an analgesic action (Drew *et al.* 2007*b*). These data suggest firstly that MA channels expressed at the soma in cultured neurons mediate mechanosensation *in vivo* and secondly that RA currents are mainly activated by light touch and SA currents by noxious mechanical stimuli.

Here we present the results of a study aimed at characterizing the encoding properties of MA currents as a function of their kinetics. We have previously used the term adapting to describe the decay of all current classes but here we provide a detailed mechanistic investigation of MA current decay and its potential physiological roles.

Our results show that RA currents display an unusual inactivation mode and that MA current kinetics are crucial in determining DRG neuron response to dynamic mechanical stimulation. Our data also highlight the importance of the molecular identity of the ion channels at the nerve terminal in shaping neuronal responses to static and repetitive mechanical stimulation.

Methods

Culture of neonatal rat neurons

Neonatal (P1) Sprague–Dawley rats were killed by decapitation in accordance with the UK Animals (Scientific Procedures) Act 1986. DRGs were removed and digested in collagenase type XI (0.6 mg ml^{-1}), protease type IX (1 mg ml^{-1}) and glucose (1.8 mg ml^{-1}) in Dulbecco's modified Eagle's medium (DMEM) for 25 min prior to mechanical trituration. Cells were then centrifuged for 5 min (190 g) and resuspended in DMEM containing 4.5 g l^{-1} glucose, 4 mM L-glutamine, 110 mg l^{-1} sodium pyruvate, 10% fetal bovine serum, 10 000 i.u. ml^{-1} penicillin–streptomycin and 100 ng ml^{-1} nerve growth factor (NGF), and plated on 35 mm dishes coated with poly-L-lysine (0.01 mg ml^{-1}) and laminin (0.02 mg ml^{-1}). Cultures were kept at 37°C in 5% CO_2. Neurons were used up to 2 days after plating.

Electrophysiology and solutions

Neurons whose soma was not in contact with those of other neurons were selected for recording. Currents were recorded using an Axopatch 200B amplifier (Molecular Devices, Sunnyvale, CA, USA). Pipettes were pulled from borosilicate glass capillaries with a P-97 puller (Sutter Instrument Co., Novato, CA, USA) and had resistances of 1–3 MΩ. The pipette solution contained (in mM): 130 potassium gluconate, 8 NaCl, 1 $CaCl_2$, 1 $MgCl_2$, 2 EGTA, 4 MgATP and 0.4 Na_2GTP (pH corrected to 7.35 using NaOH, osmolarity set to 310 mosmol l^{-1} using sucrose). For voltage dependence experiments potassium gluconate was isosmotically replaced with caesium methanesulfonate. The bath solution contained (in mM): 140 NaCl, 4 KCl, 2 $CaCl_2$, 1 $MgCl_2$ and 10 Hepes (pH 7.4 adjusted using NaOH and osmolarity 305 mosmol l^{-1} with sucrose). For $[Na^+]_o$ experiments, NaCl was replaced with *N*-methyl-D-glucamine (NMDG) and pH was adjusted with HCl. Recordings were not corrected for junction potentials and were performed at room temperature.

Currents were digitized with a Digidata 1322A data acquisition system (Molecular Devices), low pass-filtered at 2 kHz and sampled at 11 kHz. Data were recorded and stored using Clampex 8.1 (Molecular Devices). Capacitance transients were cancelled, and series resistance was compensated by at least 80%. Voltages were not corrected for liquid junction potentials. Off-line analysis, fits and statistics were performed using Clampfit 9.0 (Molecular Devices), SigmaPlot 8 (Systat Software Inc., San Jose, CA, USA) and QuickCalcs (GraphPad Software Inc., La Jolla, CA, USA). Membrane stretch-current amplitude relationships were fitted, whenever possible, with a Boltzmann equation of the form: $I(x) = I_{max}[1 + \exp(-(x - x_{1/2})/s)]^{-1}$, where I is the peak MA current amplitude at a given holding potential, x is the displacement (in micrometres) of the mechanoprobe, $x_{1/2}$ is the displacement value that produces a current density that is 50% of I_{max} and s is the current sensitivity to probe displacement. The time constants of relaxation of mechanically activated currents as well as peak current decay over time were derived from single and double exponential fits of the decaying phase of the currents according to the equation:

$$I(t) = \sum_{i=1}^{n} A i \ \exp(-t/\tau_i) + C.$$

Recovery from inactivation was fitted with an exponential equation of the form:

$$I(t) = \sum_{i=1}^{n} A i\,[1 - \exp(-t/\tau_i)] + C.$$

Values are expressed as means ± S.E.M. Difference between groups of data was assessed using the Kruskal–Wallis one-way analysis of variance test.

Mechanical stimulation

Mechanical stimulation of neuronal cell bodies was achieved using a heat-polished glass pipette (tip diameter approximately 5 μm), controlled by a piezo-electric crystal drive (Burleigh), positioned at an angle of 70 deg to the surface of the dish. The probe was positioned so that

a 10 μm movement did not visibly contact the cell but that a 12 μm stimulus produced an observable membrane deflection. Therefore a 12 μm displacement was recorded as a 2 μm displacement. The probe was moved at a speed of 0.5 μm ms^{-1} (unless otherwise stated). Series of mechanical steps in 1 or 2 μm increments were applied at 15 s intervals. Neurons that showed significant swelling as a result of repetitive mechanical stimulation were discarded (Hamill & McBride, 1997).

Results

To investigate the coding significance of the decay kinetics of mechanosensitive ion channels in DRG neurons, the stimulus probe velocity was varied to determine how the rate of mechanical stimulation affected the properties of evoked currents. These experiments revealed that rapidly adapting (RA) currents dynamically encode stimulus size and velocity whereas the magnitude of slowly adapting (SA) currents is determined primarily by the stimulus size (Fig. 1).

For these experiments, neurons were divided into three groups: those with SA currents, those with RA currents and those with currents displaying intermediate kinetics (intermediately adapting, IA). Stimuli were applied at 1, 0.5, 0.33, 0.25 and 0.17 μm ms^{-1} and the effects on peak and residual current amplitude were analysed. As shown in Fig. 1*A* and *B*, the rate of current decay is a major determinant of peak current amplitude as the probe velocity is changed: within the time frame used, current amplitude in neurons with SA currents was independent of the probe velocity whereas in neurons with RA, and to a lesser extent with IA currents, increasing the probe velocity significantly increased current amplitude. It is worth noting that very slow mechanical ramps are able to decrease SA current amplitude (see online Supplemental Material, Supplementary Fig. 1). Probe velocity did not affect the thresholds of activation in any class of currents (Fig. 1*C* and *D*). These data suggest that (1) all mechanosensitive channels open at specific thresholds, that (2) the slow decay of SA currents allows them to encode solely stimulus magnitude when the duration of stimuli is short enough for SA currents to be persistent and that (3) stimulus velocity is primarily encoded by the fast inactivating RA currents. The results are consistent with channels mediating RA currents closing soon after their activation so that at the end of longer ramps not all RA channels contribute to the peak current amplitude.

These data also suggest that IA currents result from the simultaneous activation of channels with RA and SA kinetics. In support of this, in a number of DRG neurons in which a mechanical stimulation of low amplitude generates a rapid response, further stimulation generates a slower response (Supplementary Fig. 1). Hence, for the rest of the study, we focused primarily on currents that could be classified as RA or SA currents.

To investigate the biophysical processes that underlie the dynamic properties of mechanically activated currents, we applied a series of differently patterned mechanical stimulation.

As an initial test of the mode of MA current decay we used a two-step protocol in which an initial conditioning step, of varying duration, was applied to the neuron prior to an immediate (no return to baseline) 1 μm test step (Fig. 2). It should be noted that these stimuli are of considerably longer duration ($\leq$4 s) than those used in our previous studies ($\leq$200 ms), and so revealed considerable decay in the amplitude of SA currents. In both classes of currents, as the duration of the conditioning stimulus is increased, the test pulse evokes a smaller current, indicating that both RA and SA currents undergo a time-dependent inactivation process (Fig. 2*A* and *B*). However, a clear difference was observed between the two current types: SA current amplitude decays in a homogeneous mono-exponential fashion, whereas RA current amplitude is best fitted by a double exponential, decreasing rapidly over the first 50 ms and then stabilising so that 50% of the current remains after 4 s of conditioning membrane stretch (Fig. 2*C*). Typically, although RA currents decay much more rapidly than SA currents, after about 1 s the time-dependent inactivation of a SA current is faster than the one associated with a RA current.

To determine if time-dependent inactivation accounts for the decay in current amplitude to a monophasic stimulus, we compared the decay kinetics to the decrease in peak current amplitude over time to the test pulse (Fig. 2*D*). Interestingly, the decay kinetics of SA current approximated the decrease in SA current peak amplitude (Fig. 2*D*, bottom). This suggests that inactivation accounts for the majority of current decay and that the time course of SA current inactivation is constant for a given membrane stretch, i.e. inactivation appears to be time and membrane stretch dependent. Conversely, the decrease in peak amplitude of RA currents is much slower than their decay kinetics (Fig. 2*D*, top), indicating that the kinetics of RA currents are independent on the duration of the membrane stretch. It again suggests that instead the rapid closure of RA channels takes place quickly after the channels open, pointing to an activation-dependent (rather than a time and membrane stretch dependent) mechanism.

This mechanism could also be observed when inactivation was assessed with varying stretch amplitudes and a constant duration (Fig. 3). As with increasing duration, both RA and SA currents inactivate with increasing membrane stretch (Fig. 3*A* and *B*), although as expected SA currents do so much less than RA currents, as shown by the large window current resulting from the crossing of SA current activation and inactivation curves

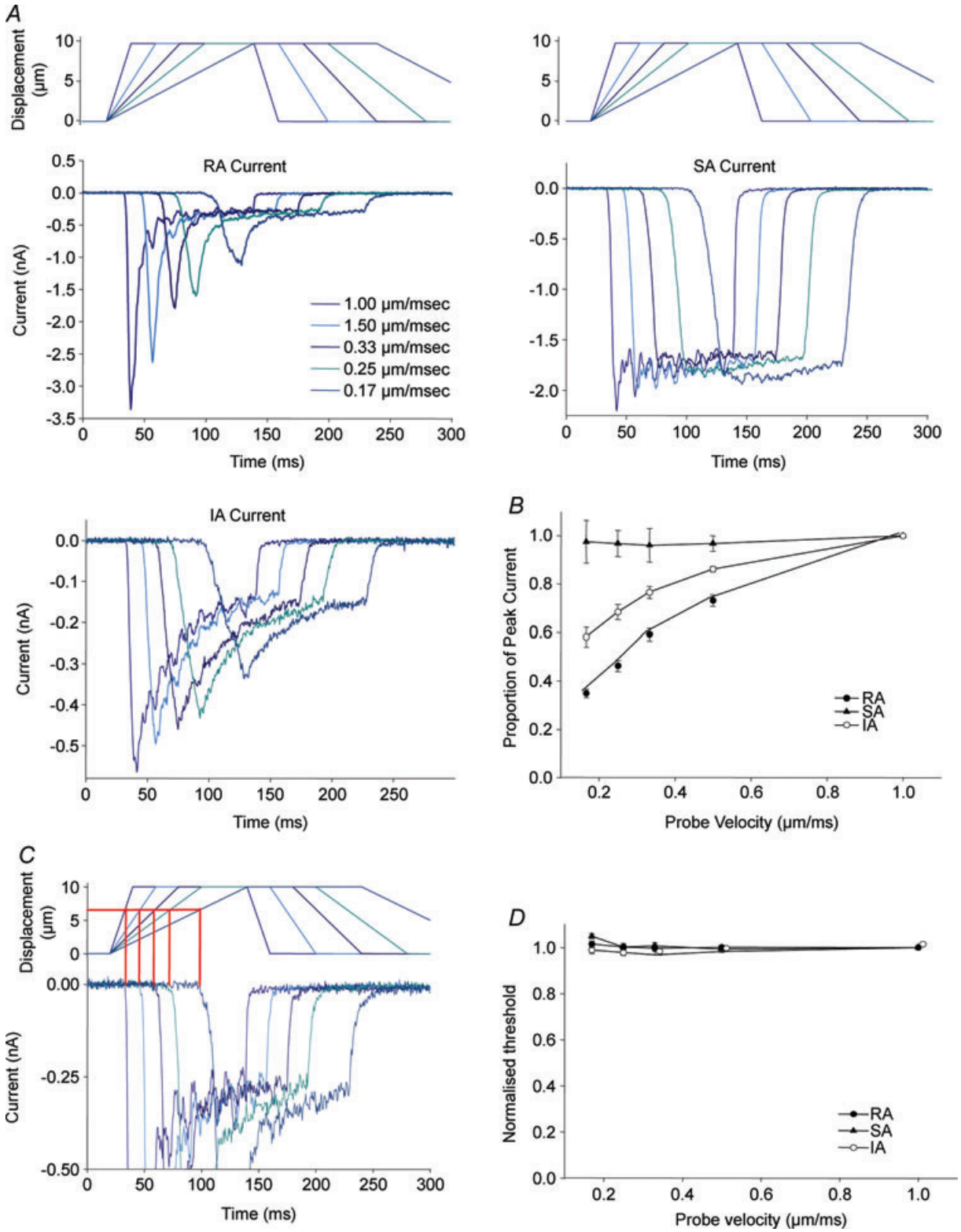

Figure 1. Effects of varying the rate of mechanical stimulation on MA current properties
A, example MA currents evoked by different probe velocities. *B*, relationship between probe velocity and MA current amplitude. RA and IA current amplitude declined as probe velocity is slowed while SA current amplitude remained unaffected. *C*, changing the rate of stimulation had no effect on current activation threshold as shown in an example in D. (RA, $n = 7$; IA, $n = 7$; SA, $n = 6$.)

(Fig. 3*B*). As expected of a stretch-dependent inactivation process, whole cell SA current inactivation becomes faster when the magnitude of the mechanical stimulation increases (Fig. 3*C*). However, again, RA current decay displays an unusual behaviour, in that the kinetics vary little with increasing membrane stretch (Fig. 3*D*). This confirms that RA current decay kinetics are not determined by the stretch of the cell membrane but rather depend on the (stretch-dependent) opening of the channel. Together, these data suggest that SA current inactivation is both time and membrane stretch dependent whereas RA current decay is stimulus dependent, and therefore indirectly membrane stretch dependent.

Physiologically mechanoreceptors are often activated by vibrational stimuli. To test the response of MA currents to vibration-like stimuli, we repetitively displaced the

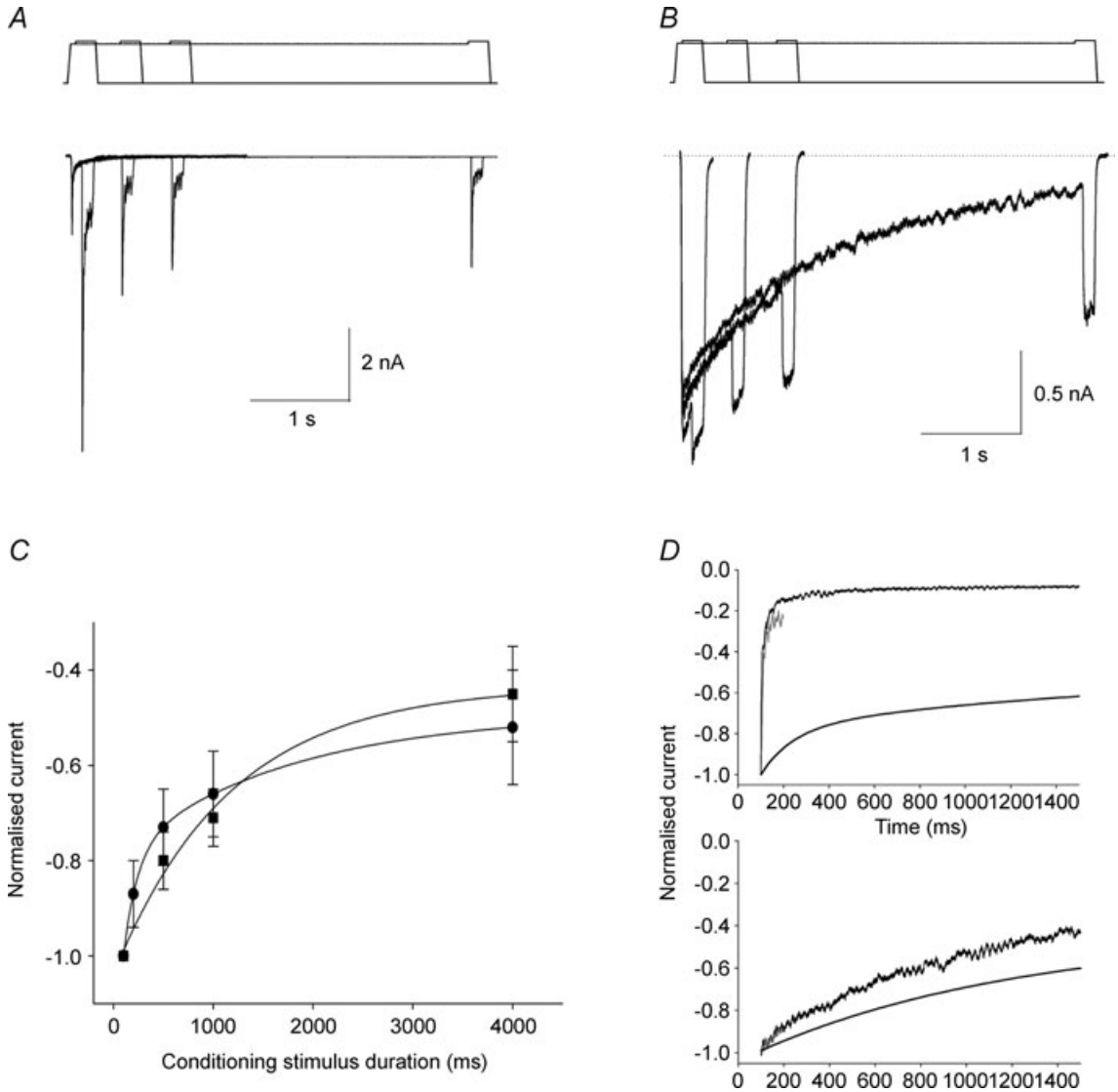

Figure 2. Time-dependent inactivation of MA currents
A, representative trace of the time-dependent decline in RA current amplitude. Currents were activated by a 4 μm conditioning stimulus of increasing duration and tested with a larger stimulus (1 μm more) without removing the conditioning stimulus. *B*, representative trace of the time-dependent decline in SA current amplitude. Same protocol as in *A*. *C*, plot of the decline in MA current amplitude depicted in *A* and *B*. Filled circles: RA currents ($n = 12$); filled squares: SA currents ($n = 6$). The decay in RA current peak current amplitude was fitted with a double exponential function with time constants $\tau_1 = 949.5 \pm 184$ ms and $\tau_2 = 35.3 \pm 4$ ms, whereas the time-dependent decrease in SA current amplitude was fitted with a single exponential function ($\tau = 1248.6 \pm 184$ ms). *D*, comparison of inactivation time courses of the conditioning current (dark trace) and the test current after 100 ms (red trace) with the mean time-dependent decay of peak current amplitude (fitted curve) for RA (top) and SA currents (bottom). Fitted curves are from *C* and inactivation time courses are from *A* and *B*.

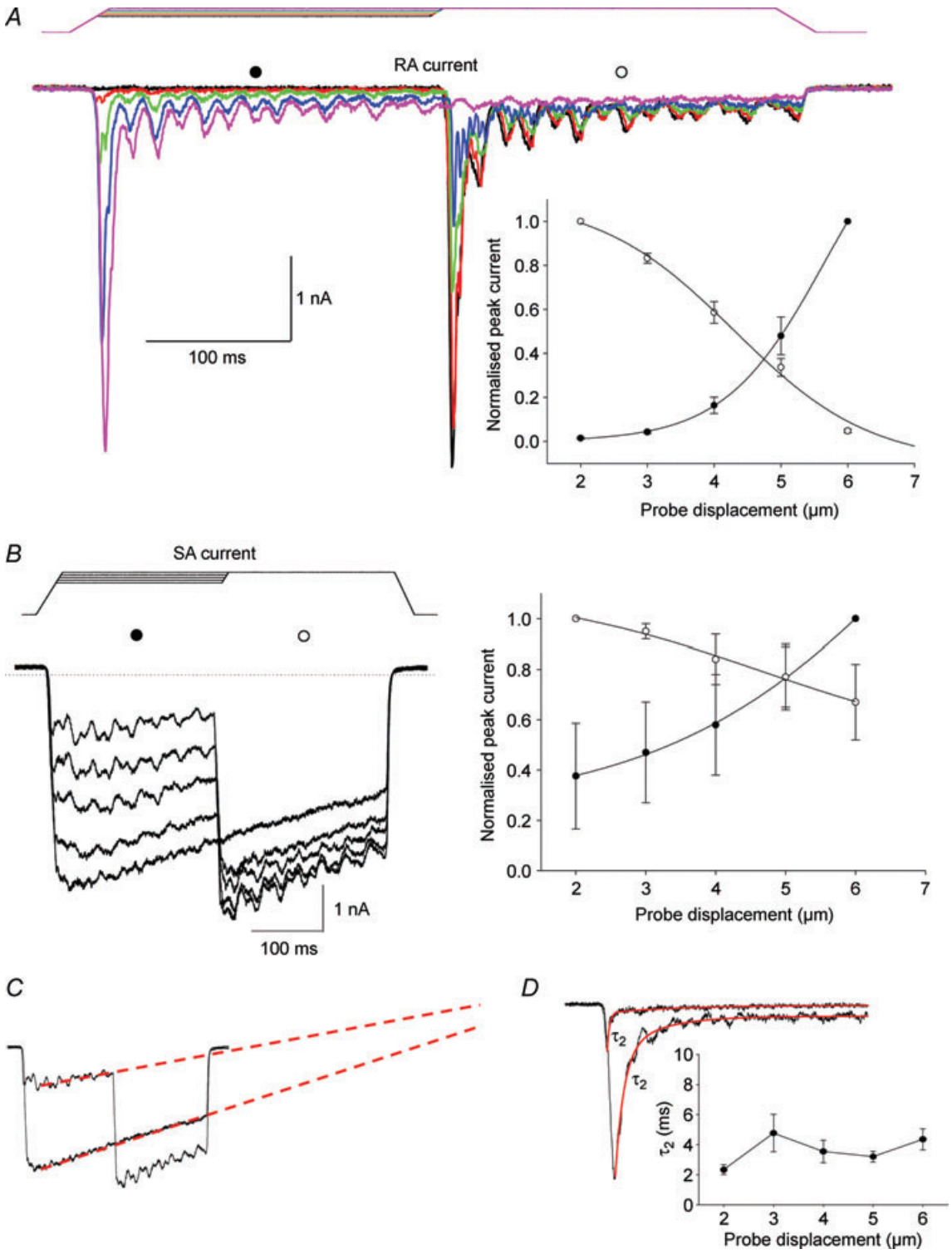

Figure 3. Membrane stretch-dependent inactivation of MA currents
A, representative trace of the membrane stretch-dependent decline in RA current amplitude. Currents were activated by a conditioning stimulus of increasing amplitude (from 2 to 6 μm) and tested with a 6 μm stimulus without removing the conditioning stimulus. Inset: mean RA current activation (filled circles) and inactivation (open circles) curves fitted to Boltzmann functions (activation: $s = 0.75$, $x_{1/2} = 4.66$ μm; inactivation: $s = -1.02$, $x_{1/2} = 3.3$ μm, $n = 8$). *B*, left, representative trace of the time-dependent decline in SA current amplitude. Currents were activated as in *A*. Right, mean SA current activation (filled circles) and inactivation (open circles) curves ($n = 5$). *C*, comparison of inactivation time courses at 1 and 5 μm for the current in *B*. Dotted red lines indicate that the

plasma membrane at a frequency of 1 Hz. This is slow when compared to the range of frequencies mechanoreceptors can detect *in vivo* (Macefield, 2005) but allowed us to observe the responses of MA currents to repetitive stimulation and did not cause damage to the neurons. We observed that SA currents are much more resilient to 1 Hz stimulations than RA currents (Fig. 4*A* and *B*). Both types of current are inactivated by repetitive stimulation in a mono-exponential fashion but whereas the magnitude of SA currents remains greater than 60% of their initial amplitude after 10 s, RA current inactivation is heavily use dependent, decreasing to approximately 20% of the initial amplitude (Fig. 4*C*). For comparison, voltage-gated Na^+ and K^+ currents in the same neurons are insensitive to 1 Hz voltage stimulations (Fig. 4*A* and *B* insets).

The fact that RA currents enter a use-dependent inactivation faster than SA currents suggests that RA currents recover from inactivation more slowly than SA currents. To test this we gave a control stimulus and then a second stimulus at increasing intervals. Figure 5 shows that recovery from inactivation is in both cases mono-exponential (Fig. 5*A* and *B*) but SA currents indeed recover on average faster than RA currents (Fig. 5*C*).

We have shown that time- and stretch-dependent channel inactivation accounts for the vast majority of current decay in SA currents but it remains unclear what mechanisms account for RA current decay whilst allowing for sensitivity to further stimulation. The discrepancy between RA current decay kinetics and time-dependent peak current amplitude decrease could be explained if the initial rapid decay in current amplitude was due to adaptation. Adaptation is the process whereby a current that decreases in amplitude over time can be reactivated without the need for the stimulus to be removed. Adaptation occurs when a current does not need to deactivate to reactivate (see Kuo & Bean, 1994), i.e. inactivation is the reaction of a channel to stimulation whereas adaptation refers to the loss of effect of the stimulus. Hamill & McBride (1992) previously described adaptation of mechanosensitive channels in *Xenopus* oocytes. To test for RA current adaptation in DRG neurons, we employed a standard adaptation protocol first used by Eatock *et al.* (1987) in hair cells of the inner ear, using a control, a conditioning and a test stimulus. Figure 6 shows representative examples of the behaviour of RA, IA and SA currents in response to this protocol. Following a conditioning stimulus, test RA (as well as IA and SA) currents are unable to return to

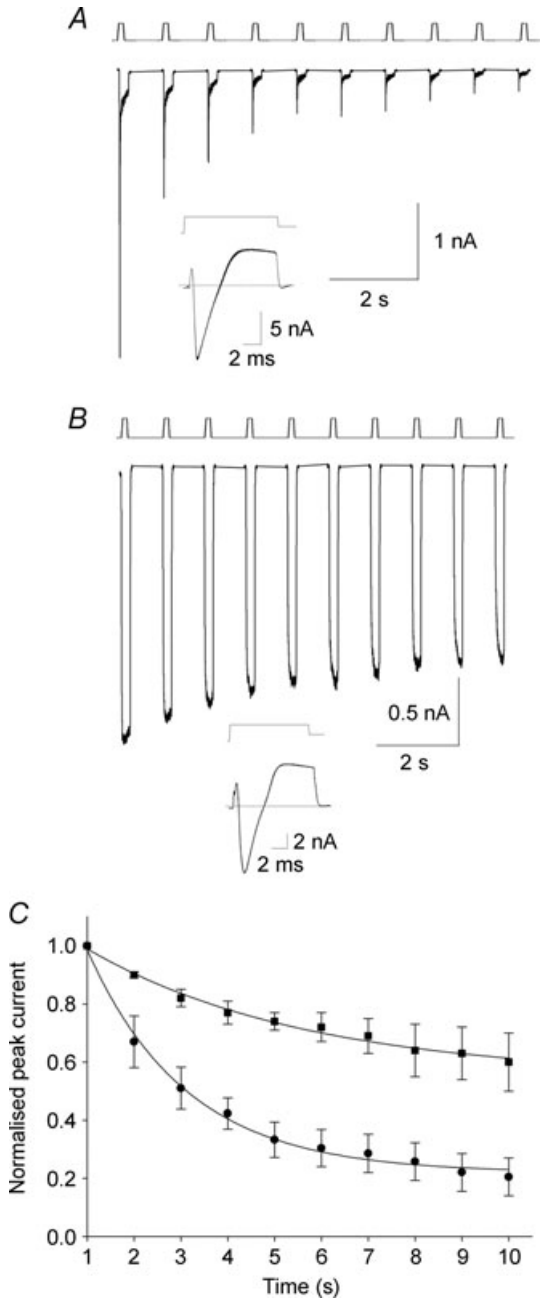

Figure 4. Use-dependent inactivation of MA currents
A, 6 μm repetitive mechanical stimulation at 1 Hz of a RA current. Inset: 1 Hz stimulation at 0 mV of inward and outward currents in the same neuron. *B*, same protocol applied to a SA current and comparison with voltage-gated currents in the same neuron (inset). *C*, use-dependent decrease in peak MA current amplitude fitted to single exponentials functions. Filled circles: RA currents ($\tau = 2.22 \pm 0.14$ s; $n = 4$); filled squares: SA currents ($\tau = 4.8 \pm 0.7$ s; $n = 4$).

rate of inactivation accelerates for increasing membrane stretch. *D*, representative RA current traces at 1 and 5 μm mechanical stimulation and their inactivation time course double exponential fits (red). Inset: relationship between the rapid decrease in peak RA current (time constant τ_2) and the amount of membrane stretch ($n = 6$). Mean τ_2 does not change with increasing membrane stretch.

preconditioning levels of activation (Fig. 6). Test RA currents are always smaller than control currents elicited 8 s before (an interval sufficient for MA currents to fully recover), even when conditioning responses are elicited by mild mechanical stimuli (Fig. 6*A*). These data demonstrate that MA currents in DRG neurons do not adapt to the stimulus and that reactivation following a conditioning step is greatest in the slowest MA currents (SA currents reactivate more than RA currents even when the former are subjected to stronger stimuli; Fig. 6).

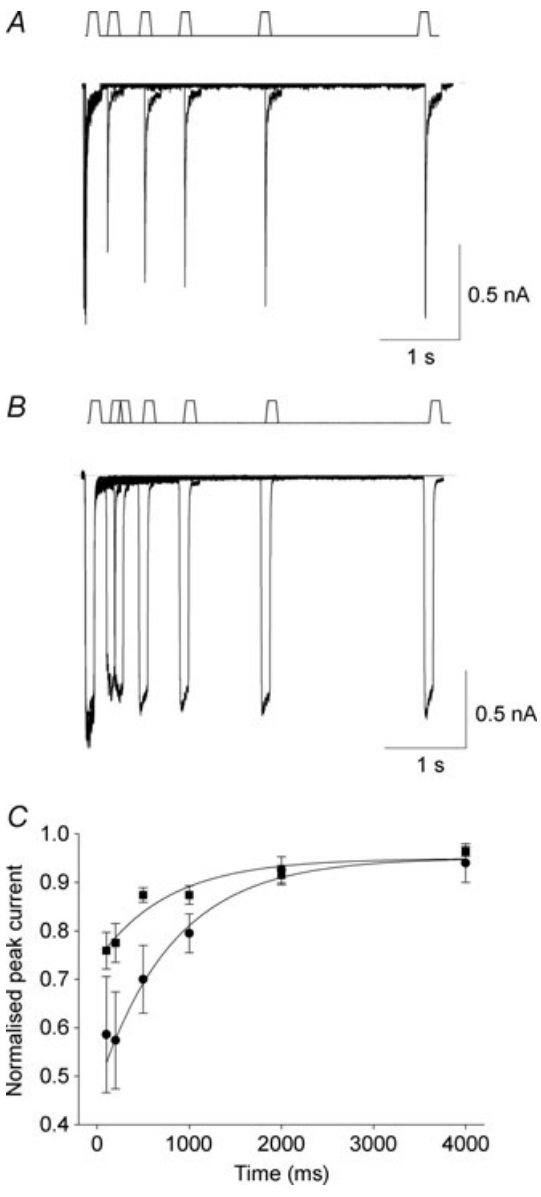

Figure 5. MA current recovery from inactivation
A, representative response of a RA current-expressing neuron mechanically stimulated by 2 consecutive stimuli at 4 μm separated by an increasing time interval. *B*, same protocol applied to a SA current. *C*, relationship between inter-stimulus interval and peak MA current fitted to single exponential functions. Filled circles: RA currents ($\tau = 811.4 \pm 70$ ms; $n = 6$); filled squares: SA currents ($\tau = 772 \pm 278$ ms; $n = 3$).

In order to shed light on the biophysical properties of MA current inactivation, we studied the decay kinetics of MA currents at different holding potentials(Fig. 7*A*). Decay of RA (Fig. 7*A*, *B*) and IA (Supplementary Fig. 2) currents was markedly voltage dependent, there being a substantial slowing of decay kinetics as the membrane potential was increasingly depolarised. Removing external Ca^{2+} did not change decay kinetics at physiological potentials (not shown), in agreement with Drew *et al.* (2002) and McCarter & Levine (2006). Furthermore, application of thapsigargin, to deplete internal Ca^{2+} stores, did not change the kinetics of either RA or SA currents (Fig. 7*C*), suggesting that MA current inactivation is insensitive to both extracellular and intracellular Ca^{2+}. As expected, removal of external Na^+ dramatically reduced the amplitude of MA currents but left their kinetics unchanged (Fig. 7*D*), demonstrating the absence of Na^+ involvement in inactivation.

Finally, we investigated the effect of MA current properties on the behaviour of DRG neurons in current clamp mode (Fig. 8). Mechanical stimulation of neurons expressing all MA current types elicited action potential firing but there were notable differences between neurons expressing RA currents and those expressing SA currents. In the latter group action potential firing was observed following stimulation with slow mechanical ramps while firing in RA current-expressing cells was more limited by the speed of the stimulation and was only observed with faster mechanical ramps (Fig. 8*A*, *B*). The lack of firing was not due to Na^+ current inactivation as slowly depolarising the same neurons in a ramp-like manner ($2\ mV\ s^{-1}$) elicited firing (Fig. 8*A* and *B*, insets). This suggests that the failure to fire with slow mechanical ramps was due to MA currents becoming too inactivated and not due to Na^+ channel inactivation, highlighting the importance of MA current kinetics on the coding of dynamic mechanical stimuli (cf. Fig. 1). Although dynamic stimuli seem to depend primarily on MA current availability, the same cannot be said of static stimulations. The absence of neuron firing throughout the static phase of mechanical stimulations suggests a reliance on voltage-gated currents. In other words, the coding of prolonged static mechanical stimuli appears to result from a fine balance between transduction currents and voltage-gated conductances expressed at the nerve terminal (modelled here in the soma). For SA current-expressing neurons a prolonged and static stimulation means a prolonged depolarisation affecting the availability of some voltage-gated channels (Na^+ channels). On the other hand, the same stimulation in the RA current-expressing cell means a rapid repolarisation that can potentially lead to very different outcomes depending on the repertoire of voltage-gated channels

expressed in the vicinity; for instance, repolarisation can result in repetitive firing if pacemaker channels of the HCN family are present or in lack of firing in the case where K^+ channels predominate. A completely opposite outcome can be witnessed in responses to repetitive stimulations (Fig. 8*C* and *D*), further reasserting the crucial role of ion channels partnering the transduction molecules at the nerve terminal.

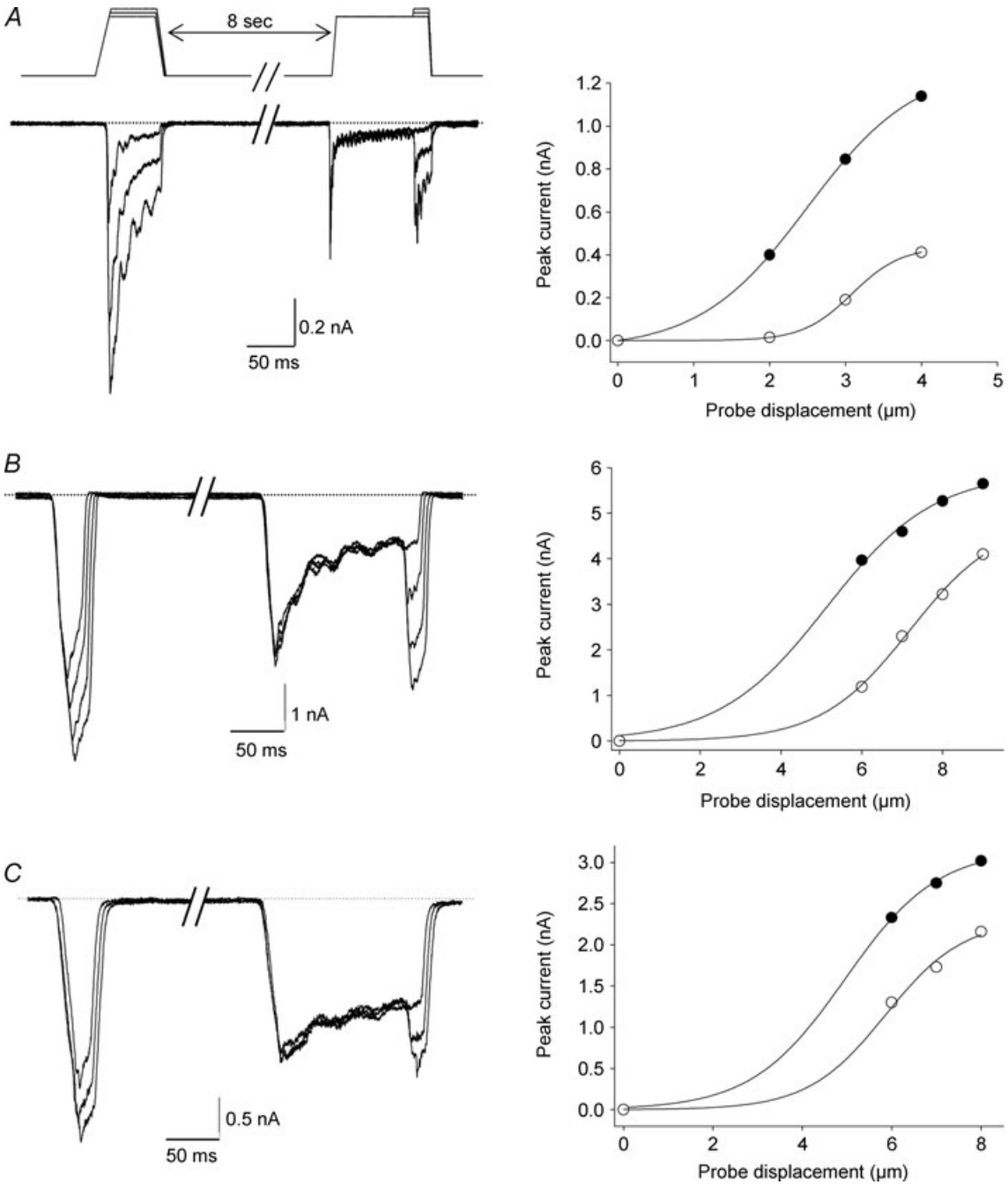

Figure 6. MA currents do not adapt to the stimulus
Left, adaptation protocol applied to RA (*A*), IA (*B*) and SA (*C*) currents. Control and conditioning currents are separated by 8 s. The conditioning current is elicited by the same amount of membrane stretch as the first control current and the 2nd and 3rd test currents are elicited by the same stimulus as the 2nd and 3rd control currents. Right, current activation curves fitted to a Boltzmann functions. Filled circles: control current; open circles: test current.

Discussion

In this study we have shown clear biophysical differences between populations of mechanosensitive ion channels in rat DRG neurons, demonstrating that distinct mechanisms determine the kinetic behaviour of different channel types. The ion channels underlying SA currents undergo a classical stimulus- and time-dependent inactivation whereas those mediating RA currents display an inactivation that is more potent when triggered by stimulus strength than time. In other words, SA currents inactivate in the presence of constant membrane stretch and recover in a time-dependent manner only when the stimulus is removed. In contrast and despite recovering more slowly, RA currents can be more easily reactivated because their decay time course is time independent, rapidly switching to a low conductance mode during the course of the stimulation.

This study confirms the existence of at least two types of MA currents that had been hypothesized from the blockade of SA currents by the peptide NMB1 (Drew *et al.* 2007*b*) and represents a first step in defining mechanisms underlying their different properties. MA currents generated by DRG neurons fall into definable categories, but they do display marked heterogeneity.

'Pure' SA currents completely lacking a RA component are rarely encountered and many MA currents classified as IA have a large component that displays very slow kinetics. Pure SA currents are currents whose time-dependent decrease in amplitude perfectly matches their inactivation kinetics. Another important implication of this work is that multiple combinations of RA and SA ion channels would determine not only the kinetics of MA currents in response to a single mechanical stimulus but also the dynamic response of a neuron to more complex stimuli.

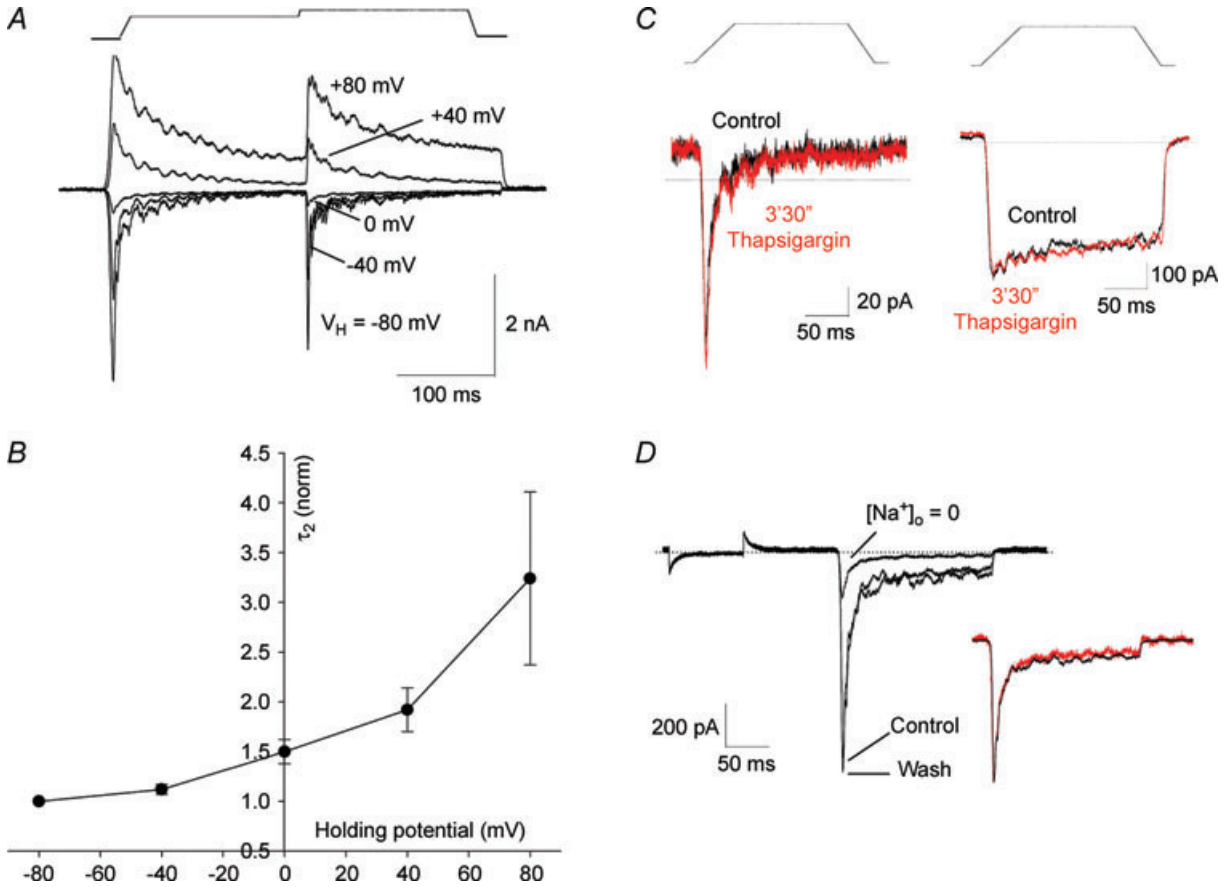

Figure 7. MA current inactivation is voltage dependent and independent of $[Ca^{2+}]_i$ and $[Na^+]_o$
A, activation of a RA current by a double stimulus protocol at various holding potentials (indicated). Leak was substracted. *B*, relationship between holding potential and the rapid phase of RA current decay (time constant τ_2). Time constants were normalised to time constant at $V_H = -80$ mV ($n = 10$ from -80 to $+40$ mV and $n = 7$ at $+80$ mV). In these experiments K^+ in the pipette solution was replaced with Cs^+. *C*, representative recording of a RA current (left) and a SA current (right) before and after 3 min 30 s of thapsigargin (1 μM) perfusion. *D*, RA current recording before and during Na^+ removal from external milieu and after wash. A hyperpolarising voltage step precedes the mechanical stimulation in order to assess series resistance changes. Inset: current trace in absence of external Na^+ (red) normalised to control trace (black).

A central issue in sensory physiology is the role played by transducer current properties in shaping the evoked pattern of sensory nerve electrical signalling. Much remains to be determined in this area for DRG neurons and it is known that auxiliary structures innervated by the peripheral nerve can filter mechanical forces impacting on the terminal (e.g. Pacinian corpuscles, Mendelson & Lowenstein, 1964; Lowenstein & Mendelson, 1965) and also that differential voltage-gated channel expression can modulate firing (e.g. Shin *et al.* 2003; Pawson *et al.* 2009). Here we show action potential firing in DRG neurons expressing different classes of mechanosensitive channels is dependent upon the type of dynamic mechanical stimulus; hence slowly increasing stimuli are more likely to be suprathreshold for action potential generation for neurons displaying SA currents than neurons expressing RA currents. On the other hand, the presence of a particular type of MA current does not guarantee a particular type of response. A strong stimulation in a SA current-expressing cell can lead to an absence of response for further stimulation whilst a smaller stimulation could allow repetitive firing. Vibratory

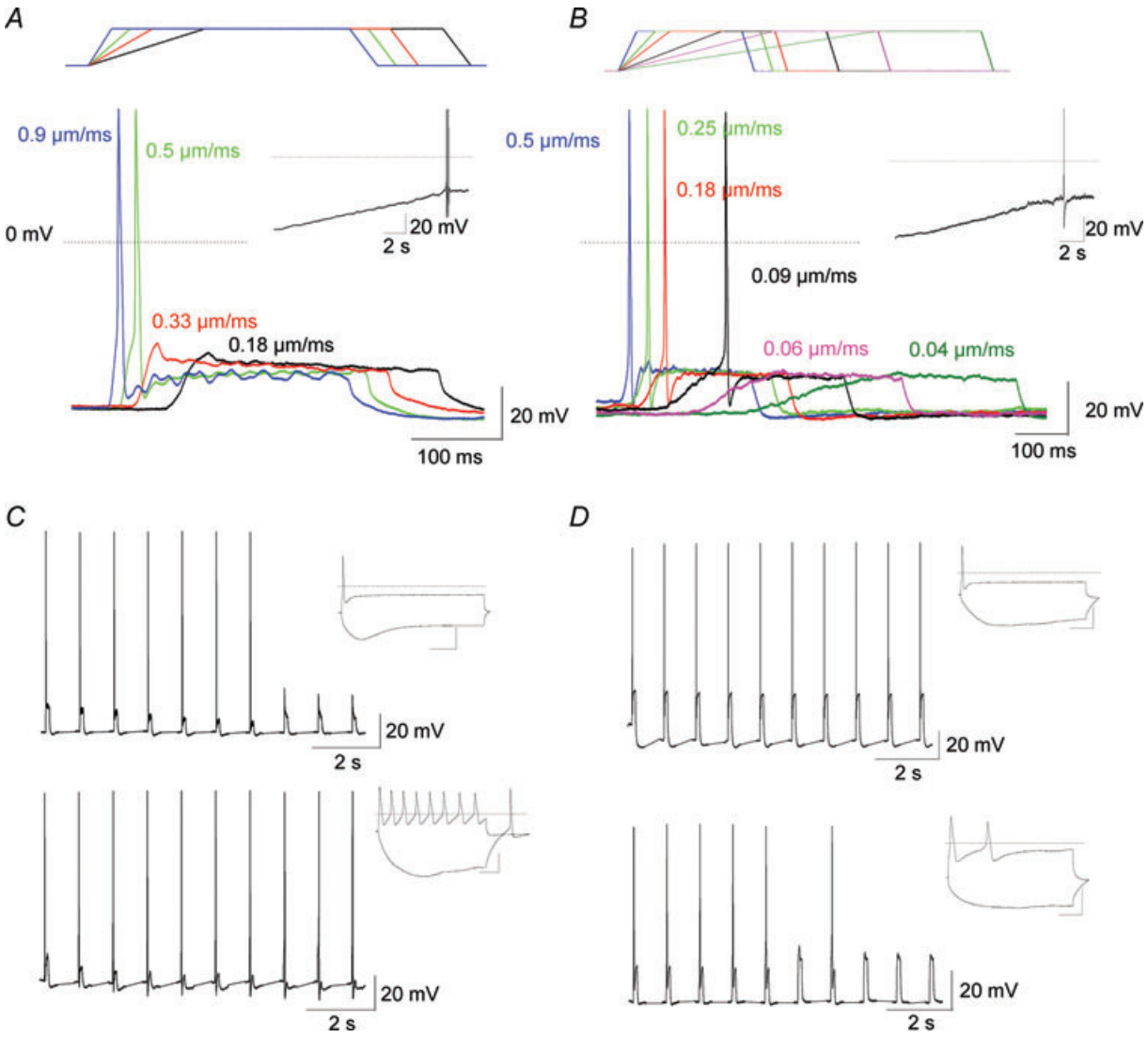

Figure 8. Diversity of mechanical responses in DRG neurons
A, action potential firing in response to different rates of mechanical stimulation in a neuron expressing a RA current. Inset: manually applied slow depolarisation of the same neuron led to action potential firing. *B*, same experiment in a neuron expressing a SA current. *C*, current clamp responses of RA current-expressing DRG neurons to 1 Hz mechanical stimulations. Top: a neuron with a pacemaker conductance and a phasic firing pattern in response to prolonged depolarisation (inset) adapts its response. Bottom: a neuron with a strong K^+-driven AHP and tonic firing pattern (inset) is able to fire action potentials indefinitely. *D*, same protocol as in *C*, in SA current-expressing neurons. A strong K^+-driven AHP allows repetitive firing whilst a lack of it leads to firing adaptation.

stimuli can also lead to different outcomes depending on the repertoire of voltage-gated (and possibly ligand-gated) channels expressed in the neuron. This is in agreement with several studies that showed that neuronal responses result from a complicated web of conductance interactions and demonstrate that transducer currents are part of a much bigger functional complex when cellular responses to stimuli are considered (Bean, 2009; George *et al.* 2009; Pawson *et al.* 2009; Taylor *et al.* 2009). Amongst others, ion channels such as cyclic nucleotide-gated HCN channels (Momin *et al.* 2008), M and A-type K^+ channels (Linley *et al.* 2008; Phuket & Covarrubias, 2009) as well as Ca^{2+}-activated Cl^- channels (Boudes *et al.* 2009) are very likely to play a crucial role in mechanical stimuli transduction.

A large body of work has described mechanosensitive ion channels in a number of cell types, including both receptor cells of sensory systems and cells in non-sensory tissues. The best-characterised mechanosensory channel type is that of cochlea hair cells that detect head movements and sound waves via deflections of their stereocilia. These ion channels adapt to constant mechanical stimuli, that is the channels change their gating sensitivity in order to be able to reactivate with further stimulation, an observation confirmed in every species investigated: turtle (Crawford *et al.* 1989), bullfrog (Eatock *et al.* 1987; Shepherd & Corey, 1994), mouse (Holt *et al.* 1997) and rat (Kennedy *et al.* 2003). In this cell type two types of adaptation are present; a rapid one, mediated by Ca^{2+} influx (Ricci *et al.* 2005) and a slow one involving the actin-dependent molecular motor myosin-1c (Vollrath *et al.* 2007). Interestingly, in DRG neurons inactivation is independent of Ca^{2+}, suggesting a key mechanistic difference between mechanosensitive channel adaptation in cochlear hair cells and inactivation in DRG neurons. Therefore, it appears that the terms 'RA', 'IA' and 'SA' that we have used so far to describe MA currents in DRG neurons are inadequate. Nevertheless, as a matter of simplicity, and as decay mechanisms for 'RA' currents remain incompletely understood, we propose not to change it. A common characteristic of adaptation and inactivation is that in both DRG neurons and hair cells (Assad *et al.* 1989; Ricci *et al.* 2005) current decay is voltage dependent, although the physiological relevance of this is unclear.

Adaptation is also observed in *Drosophila* mechanosensory bristles, where mechanotransduction is mediated (at least in part) by the nompC channel (Walker *et al.* 2000), and in mechanosensitive ion channels of *Xenopus* oocytes (Hamill & McBride, 1992). However, studies of stretch-activated cation channels of rat astrocytes (Suchyna *et al.* 2004) and the ubiquitously expressed mechano-gated K2P channels (Honoré *et al.* 2006) have shown that these channels do not adapt to mechanical stimuli but, instead, inactivate. Therefore, it appears that two distinct types of mechanosensitive channels can be distinguished: (1) a ubiquitously expressed population of stretch-activated, GsMTx-4-sensitive channels (Suchyna *et al.* 2000) expressed in non-sensory organs (such as astrocytes and myocytes) that do not adapt to a sustained stimulus and (2) a class of mechanotransducing ion channels expressed in sensory organs (e.g. cochlea hair cells, bristles) that show adaptation.

The results presented here suggest that DRG neurons express a class of RA mechanosensitive ion channels with unique features. Like K2P channels, RA currents in DRG neurons do not adapt to the stimulus, but contrary to K2P channels, MA current kinetics do not change with increasing stretch, nor do they inactivate in a mono-exponential fashion, strongly suggesting that the mechanism of MA current inactivation in DRG neurons is different from the inactivation process in K2P channels (Honoré *et al.* 2006).

As discussed above, the firing properties depend on many different parameters but because RA currents are the dominant form of MA current in large DRG neurons associated primarily with low threshold mechanoreception (Drew *et al.* 2002, 2007*b*; Hu & Lewin, 2006), it is very likely that their kinetic properties are designed to best fit this sensory modality. RA currents, by preventing action potential firing upon slowly increasing mechanical stimulation, are best designed to encode the rapid, brisk stimuli associated with innocuous touch.

In contrast nociceptive neurons express a class of slowly inactivating mechanosensitive ion channels and these channels allow action potential firing for slow stimulations and henceforth may better encode the extent of tissue compression rather than dynamic aspects of the stimulus.

This study used endogenous currents in cultured DRG neurons as a model of the peripheral transducing terminal. When the molecular identities of the underlying ion channels have been uncovered, biophysical studies will be greatly facilitated and the critical structural domains mediating activation and inactivation can be resolved.

References

Assad JA, Hacohen N & Corey DP (1989). Voltage dependence of adaptation and active bundle movement in bullfrog saccular hair cells. *Proc Natl Acad Sci U S A* **86**, 2918–2922.

Bean BP (2009). Inhibition by an excitatory conductance: a paradox explained. *Nat Neurosci* **12**, 530–532.

Boudes M, Sar C, Menigoz A, Hilaire C, Péquignot MO, Kozlenkov A, Marmorstein A, Carroll P, Valmier J & Scamps F (2009). Best1 is a gene regulated by nerve injury and required for Ca^{2+}-activated Cl^- current expression in axotomized sensory neurons. *J Neurosci* **29**, 10063–10071.

Crawford AC, Evans MG & Fettiplace R (1989). Activation and adaptation of transducer currents in turtle hair cells. *J Physiol* **419**, 405–434.

Drew LJ, Wood JN & Cesare P (2002). Distinct mechanosensitive properties of capsaicin-sensitive and -insensitive sensory neurons. *J Neurosci* **22**, RC228.

Drew LJ, Rohrer DK, Price MP, Blaver KE, Cockayne DA, Cesare P & Wood JN (2004). Acid-sensing ion channels ASIC2 and ASIC3 do not contribute to mechanically activated currents in mammalian sensory neurones. *J Physiol* **556**, 691–710.

Drew LJ & Wood JN (2007*a*). FM1-43 is a permeant blocker of mechanosensitive ion channels in sensory neurons and inhibits behavioural responses to mechanical stimuli. *Mol Pain* **3**, 1.

Drew LJ, Rugiero F, Cesare P, Gale JE, Abrahamsen B, Bowden S, Heinzmann S, Robinson M, Brust A, Colless B, Lewis RJ & Wood JN (2007*b*). High-threshold mechanosensitive ion channels blocked by a novel conopeptide mediate pressure-evoked pain. *PLoS ONE* **2**, e515.

Eatock RA, Corey DP & Hudspeth AJ (1987). Adaptation of mechanoelectrical transduction in hair cells of the bullfrog's sacculus. *J Neurosci* **7**, 2821–2836.

George MS, Abbott LF & Siegelbaum SA (2009). HCN hyperpolarization-activated cation channels inhibit EPSPs by interactions with M-type K^+ channels. *Nat Neurosci* **12**, 577–584.

Hamill OP & McBride DW Jr (1992). Rapid adaptation of single mechanosensitive channels in *Xenopus* oocytes. *Proc Natl Acad Sci U S A* **89**, 7462–7466.

Hamill OP & McBride DW Jr (1997). Induced membrane hypo/hyper-mechanosensitivity: a limitation of patch-clamp recording. *Annu Rev Physiol* **59**, 621–631.

Holt JR, Corey DP & Eatock RA (1997). Mechanoelectrical transduction and adaptation in hair cells of the mouse utricle, a low-frequency vestibular organ. *J Neurosci* **17**, 8739–8748.

Honoré E, Patel AJ, Chemin J, Suchyna T & Sachs F (2006). Desensitization of mechano-gated K2P channels. *Proc Natl Acad Sci U S A* **103**, 6859–6864.

Hu J & Lewin GR (2006). Mechanosensitive currents in the neurites of cultured mouse sensory neurones. *J Physiol* **577**, 815–828.

Kennedy HJ, Evans MG, Crawford AC & Fettiplace R (2003). Fast adaptation of mechanoelectrical transducer channels in mammalian cochlear hair cells. *Nat Neurosci* **6**, 832–836.

Kuo CC & Bean BP (1994). Na^+ channels must deactivate to recover from inactivation. *Neuron* **12**, 819–829.

Lewin GR & Moshourab R (2004). Mechanosensation and pain. *J Neurobiol* **61**, 30–44.

Linley JE, Rose K, Patil M, Robertson B, Akopian AN & Gamper N (2008). Inhibition of M current in sensory neurons by exogenous proteases: a signalling pathway mediating inflammatory nociception. *J Neurosci* **28**, 11240–11249.

Lowenstein WR & Mendelson M (1965). Components of receptor adaptation in a Pacinian corpuscle. *J Physiol* **177**, 377–397.

Macefield VG (2005). Physiological characteristics of low-threshold mechanoreceptors in joints, muscle and skin in human subjects. *Clin Exp Pharmacol Physiol* **32**, 135–144.

McCarter GC & Levine JD (2006). Ionic basis of a mechanotransduction current in adult rat dorsal root ganglion neurons. *Mol Pain* **2**, 28.

Mendelson M & Lowenstein WR (1964). Mechanisms of receptor adaptation. *Science* **144**, 554–555.

Momin A, Cadiou H, Mason A & McNaughton PA (2008). Role of the hyperpolarization-activated current I_h in somatosensory neurons. *J Physiol* **586**, 5911–5929.

Pawson L, Prestia LT, Mahoney GK, Güçlü B, Cox PJ & Pack AK (2009). GABAergic/glutamatergic-glial/neuronal interaction contributes to rapid adaptation in pacinian corpuscles. *J Neurosci* **29**, 2695–2705.

Phuket TR & Covarrubias M (2009). Kv4 channels underlie the subthreshold-operating A-type K-current in nociceptive dorsal root ganglion neurons. *Front Mol Neurosci* **2**, 3.

Ricci AJ, Kennedy HJ, Crawford AC & Fettiplace R (2005). The transduction channel filter in auditory hair cells. *J Neurosci* **25**, 7831–7839.

Rugiero F & Wood JN (2009). The mechanosensitive cell line ND-C does not express functional thermoTRP channels. *Neuropharmacology* **56**, 1138–1146.

Shepherd GM & Corey DP (1994). The extent of adaptation in bullfrog saccular hair cells. *J Neurosci* **14**, 6217–6229.

Shin JB, Martinez-Salgado C, Heppenstall PA & Lewin GR (2003). A T-type calcium channel required for normal function of a mammalian mechanoreceptor. *Nat Neurosci* **6**, 724–730.

Suchyna TM, Johnson JH, Hamer K, Leykam JF, Gage DA, Clemo HF, Baumgarten CM & Sachs F (2000). Identification of a peptide toxin from *Grammostola spatulata* spider venom that blocks cation-selective stretch-activated channels. *J Gen Physiol* **115**, 583–598.

Suchyna TM, Besch SR & Sachs F (2004). Dynamic regulation of mechanosensitive channels: capacitance used to monitor patch tension in real time. *Phys Biol* **1**, 1–18.

Taylor AL, Goaillard JM & Marder E (2009). How multiple conductances determine electrophysiological properties in a multicompartment model. *J Neurosci* **29**, 5573–5586.

Vollrath MA, Kwan KY & Corey DP (2007). The micromachinery of mechanotransduction in hair cells. *Annu Rev Neurosci* **30**, 339–365.

Walker RG, Willingham AT & Zuker CS (2000). A *Drosophila* mechanosensory transduction channel. *Science* **287**, 2229–2234.

Author contributions

All experiments were performed in the Molecular Nociception Group, UCL. F.R., L.J.D. and J.N.W. conceived and designed the experiments; F.R. and L.J.D. collected, analysed and interpreted the data; and F.R., L.J.D. and J.N.W. drafted, critically revised and approved the final version of the article.

Acknowledgements

Our work is supported by a WCU grant R31-2008-000-10103-0 and by the BBSRC, MRC and Wellcome Trust.

Authors' present addresses

L. J. Drew: Department of Physiology and Cellular Biophysics, Columbia University, New York, New York, USA.

J. N. Wood: World class University Programme, Department of Molecular Medicine and Biopharmaceutical Chemistry, Seoul National University, Seoul 151-742, Korea.